Insulin Amyloid Fibrils: An Excellent Platform for Controlled Synthesis of Ultrathin Superlong Platinum Nanowires with High Electrocatalytic Activity

Longgai Zhang,[†] Na Li,[†] Faming Gao,* Li Hou, and Ziming Xu

Key Laboratory of Applied Chemistry, Yanshan University, Qinhuangdao 066004, P. R. China

ⓈSupporting Information

ABSTRACT: Highly uniform single-crystal ultrathin Pt nanowires (UTPtNWs) with a diameter of ∼1.8 nm and a superhigh aspect ratio of $>10^4$ were fabricated using insulin amyloid fibrils (INSAFs) as sacrificial templates. The use of INSAFs to build the UTPtNWs allowed for the preferential exposure of low-energy crystal facets that would be highly advantageous for the methanol oxidation reaction. The UTPtNWs displayed a large electrochemical active surface area of 71.34 m²/g, which is much higher than that of a commercial Pt/C catalyst. The UTPtNWs also maintained excellent electrochemical durability under repeated cyclic voltammetry scans. Because of its exciting high electrochemical activity, UTPtNWs is a promising material for the design of next-generation electrocatalysts and would also be useful in sensing, biomedical, and other electrochemical applications.

Platinum nanostructures with various sizes and shapes have been intensively investigated because of their broad range of potential applications, including as highly active catalysts in many chemical reactions,[1] as gas sensors,[2] and as electrode materials in fuel cells.[3] Among various applications, electrocatalysts in fuel cells and related applications primarily consist of Pt nanoparticles. Nevertheless, a primary challenge with the use of Pt nanoparticle electrocatalysts is that these zero-dimensional morphologies possess proportionally larger numbers of lattice boundaries, defect sites, and low-coordination atoms at their surfaces.[4] Therefore, the production of Pt nanoparticle catalyst with great catalytic performance and utilization efficiency is still costly and far from trivial. Controlling the morphology of Pt nanostructures can provide a great opportunity to increase their activity and improve their catalytic properties on a mass basis. Not surprisingly, one-dimensional (1D) nanostructures such as Pt nanowires (NWs) possess (a) higher aspect ratios, (b) fewer defect sites, (c) fewer lattice boundaries, and (d) higher numbers of surface atoms, all of which are desirable attributes for fuel cell catalysts.[5] In addition, 1D structures maintain improved electron transport characteristics as a result of the path-directing effects of the structural anisotropy.[6] In this sense, the ability to control the synthesis of ultrathin Pt NWs (UTPtNWs) with superhigh aspect ratios will play an important role in the design of next-generation electrocatalysts.

Recent years have seen an explosive interest in the synthesis of UTPtNWs. Dodelet and co-workers synthesized UTPtNWs grown directly on the nanospheres of a carbon black.[7] Most of the Pt NWs were ca. 4 nm in width, and 10−30 nm in length. Further improvements were observed by Sun and co-workers, who synthesized UTPtNWs on nitrogen-doped carbon nanotubes that displayed diameters of ca. 2.5 nm and lengths of up to 100 nm.[8] Moreover, Wong and co-workers synthesized UTPtNWs with a diameter of ca. 1.8 nm and lengths of up to 100 nm, and their as-prepared UTPtNWs showed higher electrocatalytic performance.[3b] Nevertheless, despite these tangible improvements in the synthesis of UTPtNWs and the enhancement of their catalytic activity, the synthesis of UTPtNWs with superhigh aspect ratios, which could afford even more highly active catalysts while simultaneously minimizing the precious metal loading, is still challenging. In this paper, therefore, we report on the synthesis, characterization, and electrocatalytic activity of high-quality UTPtNWs with an average diameter of only 1.8 nm and a very high aspect ratio of at least 10^4 using insulin amyloid fibrils (INSAFs) as sacrificial templates.

The INSAFs can be achieved simply in vitro under conditions of low pH and high temperature.[9] INSAFs feature characteristics common to all amyloids. The highly flexible structures of soluble monomers and dimers rapidly convert to form amyloid fibers when they associate with preformed fibers that act as seeds for fiber formation.[9b,10] The fibers can grow by extension up to lengths in the micrometer range. INSAFs have several properties that make them amenable to the manufacturing process. Once the fibers are formed, they have higher than average chemical stability, as demonstrated by the fact that they can even withstand diverse metallization procedures.[9d−g] In addition, the selected amide sites on INSAFs can recognize and interact with inorganic substrates. These excellent characteristics led us to investigate the use of INSAFs as scaffolds to control the synthesis of UTPtNWs.

We prepared INSAFs by a modification of the method previously reported by Jansen and co-workers,[9b] using insulin powder from bovine pancreas without further purification. This polymerization process resulted in INSAFs with a narrow diameter distribution and lengths of several micrometers, as shown in the transmission electron microscopy (TEM) image in Figure S1 in the Supporting Information. INSAFs were directly detected by TEM without negative staining. After the polymerization process, the INSAFs were incubated with
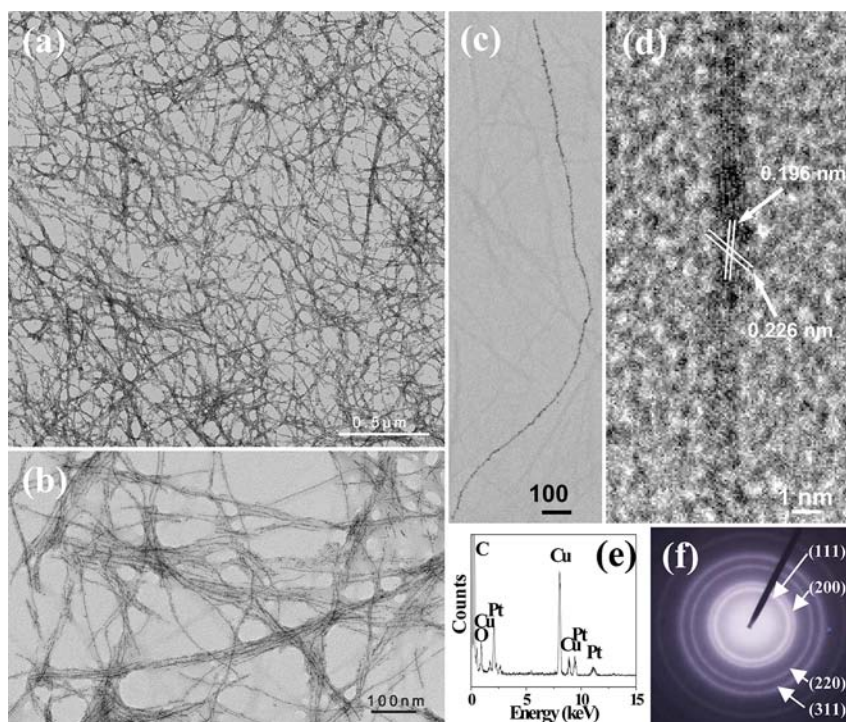
Figure 1. (a) Low- and (b) high-magnification TEM images of UTPtNWs. (c) TEM image of a typical single Pt nanowire. (d) HRTEM image of a single Pt nanowire. (e) EDS spectrum and (f) SAED pattern of UTPtNWs built using INSAFs.

$[PtCl_x]^{4-x}$ complexes (where $[PtCl_x]^{4-x}$ represents all orders of solvolysis products of H_2PtCl_6) in aqueous solution, and the $[PtCl_x]^{4-x}$ were subsequently reduced by addition of a reducing agent to obtain UTPtNWs. We have elaborated a possible detailed mechanism of UTPtNW growth using INSAFs as scaffolds, hoping it will guide directions for future research (see the SI for more details).

In our studies, the crystallinity and purity of the as-prepared UTPtNWs were studied by means of powder X-ray diffraction (PXRD) (Figure S2). The diffraction peaks could be readily indexed to the (111), (200), (220), and (311) reflections of face-centered cubic (fcc) platinum (JCPDS no. 87-0647), indicating that Pt exists in the form of a crystalline state. The diffraction peak at $2\theta = 24.0°$ corresponds to the INSAFs. No detectable impurity peaks were observed in the PXRD pattern. In particular, all of the diffraction peaks were broadened, indicating nanoscale structural features.

TEM measurements were carried out on the metallized INSAFs. The TEM images in Figure 1a,b show the UTPtNWs at different magnifications. The low-magnification TEM image (Figure 1a) reveals the presence of abundant 1D UTPtNWs with lengths of several tens to hundreds of micrometers intertwisted with each other to form NW networks. The high-yield production of UTPtNWs demonstrated that the observed features are indeed representative. A higher-magnification image is shown in Figure 1b. As the dominant form, the aligned UTPtNWs had a uniform diameter along their entire length, which was in the range of micrometers. A typical single Pt NW selected randomly is shown in Figure 1c. This nanowire had a uniform diameter of ca. 1.8 nm with a length of ca. 2.1 μm, corresponding to an aspect ratio of >10^4, which therefore indicates the UTPtNWs prepared by this simple method could yield aspect ratios of 10^4 or higher. In addition, energy-dispersive X-ray spectroscopy (EDS) was performed on a random selection of UTPtNWs, showing these UTPtNWs to

be composed only of platinum (Figure 1e). The C and Cu signals arose from the TEM grid. The selected-area electron diffraction (SAED) pattern recorded from a few UTPtNWs confirmed their high crystallinity (Figure 1f). The values in the SAED pattern correspond to the (111), (200), (220), and (311) planes of the expected fcc Pt structure, consistent with the XRD results. Besides the ultrathin nature, these UTPtNWs were also single-crystalline. A high-resolution TEM (HRTEM) image taken from an individual Pt nanowire showed that this nanowire had an average diameter of ca. 1.5 nm, and the lattice spacings of 0.226 and 0.196 nm are consistent with the {111} and {200} lattice planes in fcc Pt (Figure 1d). Both the HRTEM images and SAED patterns confirmed that the axis of the nanowire was along the ⟨111⟩ direction and that the nanowire was structurally uniform, and no dislocation was detected in the examined area. To the best of our knowledge, this is the first time that single-crystalline Pt NWs with such thin diameters and high aspect ratios have been synthesized with such a simple method.

This incredible 1D motif possesses advantageous intrinsic structural aspects that should impart improved catalytic performance. This is of interest for electrocatalytic industrial applications. Cyclic voltammetry was used to study the electrochemical properties of UTPtNWs. The obtained UTPtNWs were supported on a bare glassy carbon electrode (GCE). The electrodes were immersed in deoxygenated 0.5 M H_2SO_4 solution, and the potential was scanned from −0.25 to 1.15 V at a scan rate of 50 mV/s to obtain cyclic voltammograms (CVs). As shown in Figure 2, almost no redox behavior was observed on GCE. Commercial Pt/C displayed an enhanced activity in comparison with that found with GCE. In comparison with commercial Pt/C and GCE, the shape of the UTPtNWs CV shows characteristics similar to those of Pt, indicating that Pt NWs were effectively loaded on the GCE. The electrochemical active surface area (ECSA)
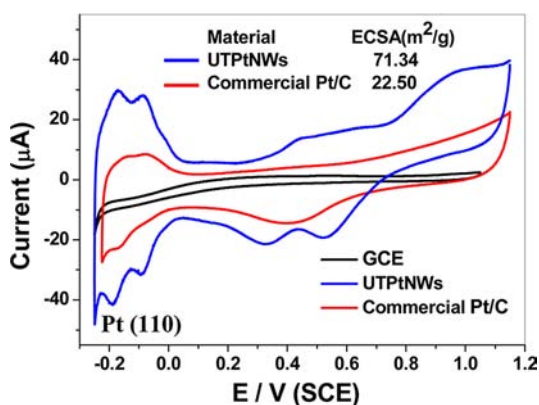
Figure 2. CVs of GCE, UTPtNWs, and a commercial Pt/C catalyst in 0.5 M H_2SO_4 solution at a scan rate of 50 mV/s.

provides important information regarding the number of available active sites, with a higher ECSA indicating that more electrochemical active sites exist. The region for hydrogen desorption is commonly used to estimate the ECSA. The UTPtNWs displayed an outstandingly high ECSA of 71.34 m^2/g, which is much higher than that of the commercial Pt/C catalyst (22.50 m^2/g). The significantly larger value is strong evidence that the UTPtNWs possess a much larger number of electrochemical active sites, making it a promising material for electrochemical applications.

In addition, the variation in the shapes of CV curves suggests the exposure of different catalytic facets on the surfaces of the various nanostructures. The CV curve in Figure 2 showed the standard hydrogen adsorption potential of −0.16 V vs SCE for the (110) facet of Pt.[11] The variation in catalytic activitys can also be attributed to different exposed facets of Pt nanostructures. It is known that the rate of methanol oxidation is highest on Pt{110} among the low-index surfaces when using H_2SO_4 as the electrolyte.[12] The more exposed {110} surface on Pt NWs would lead to higher activity in the methanol oxidation reaction (MOR). Accordingly, the MOR activities of the UTPtNWs and the commercial Pt/C catalyst were determined using cyclic voltammetry (Figure 3) in the presence of 1 M methanol in a 0.5 M H_2SO_4 electrolyte. The current density (J) was calculated to correspond directly to the catalytic activity of unit surface area (Pt) of the sample. Thus, it can be directly compared for different samples. There are two oxidation peaks
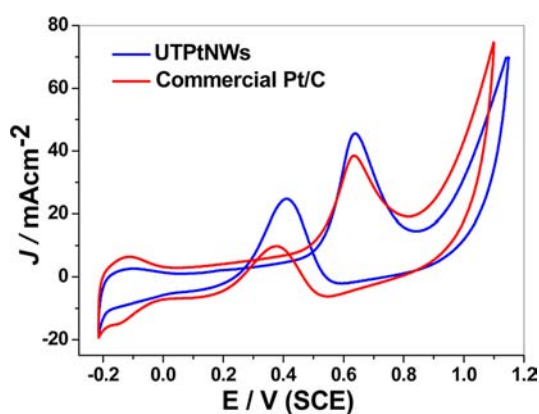
for methanol oxidation over UTPtNWs and the commercial Pt/C catalyst, i.e., at ca. 0.64 V vs SCE for the forward peak and ca. 0.40 V for the backward peak. The UTPtNWs display higher current density values than that of the commercial Pt/C catalyst throughout. The forward peak current density for the UTPtNWs is 45.50 mA cm^{-2}, which is 18% higher than that for the commercial Pt/C catalyst (38.50 mA cm^{-2}), suggesting a higher MOR activity of UTPtNWs. The higher specific activity of UTPtNWs might be due to the preferential exposure of certain crystal facets and/or to the presence of fewer surface defects on the UTPtNWs, allowing the UTPtNWs to exhibit even higher MOR activities.

To probe the stability of UTPtNWs further, the UTPtNWs were examined by repetitive scans in a 0.5 M H_2SO_4 solution. The UTPtNWs maintained 74% of the initial current after 1000 cycles, whereas the commercial Pt/C catalyst retained only 13.5% of its initial current after 500 cycles. Representative TEM images of UTPtNWs before and after 1000 cycles are shown in Figure S4c,d. As expected, the long NWs were converted largely into wire fragments. In contrast, the TEM images of the commercial Pt/C catalyst (Figure S4a,b) showed a rapid decrease of Pt nanoparticles after 500 cycles. On the basis of the morphology after repetitive CV scans, the higher remaining currents of UTPtNWs can be attributed largely to the residual Pt nanowires, in support of the result that the UTPtNWs are more stable than commercial Pt/C catalyst under repeated CV scanning. Furthermore, UTPtNWs still maintained a steady-state current that was 90% of the initial current after storage at 4 °C for more than 10 days. The slight reduction in the current in the CV after preservation of the UTPtNWs for a long time further proved their excellent stability. Therefore, this anisotropic structure makes the UTPtNWs uniquely advantageous as electrocatalysts for long-term applications in fuel cells because of their durability.

Typical CVs recorded for the UTPtNWs in 0.5 M H_2SO_4 at different scan rates ranging from 20 to 350 mV/s are shown in Figure 4. An increase in the current with increasing scan rate was observed for UTPtNWs. Meanwhile, the peak shape of the CVs showed a relatively reversible electrochemical reaction, allowing a sufficiently fast electron transfer rate for good electroanalytical performance. At all of the scan rates, the UTPtNWs exhibited excellent electrochemical performance. Plots of the anodic and cathodic peak currents versus the
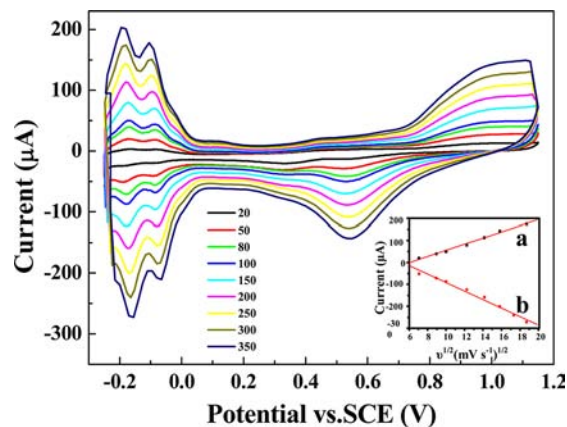

Figure 3. CVs of UTPtNWs and a commercial Pt/C catalyst in a mixture of 0.5 M H_2SO_4 and 1 M CH_3OH solution at a scan rate of 50 mV/s.

Figure 4. CVs of UTPtNWs in 0.5 M H_2SO_4 at different scan rates. The inset shows plots of (a) anodic and (b) cathodic peak currents vs the square root of the scan rate ($v^{1/2}$) for UTPtNWs.

11328

dx.doi.org/10.1021/ja302959e | J. Am. Chem. Soc. 2012, 134, 11326−11329

square root of the scan rate ($v^{1/2}$) for UTPtNWs are also given in the Figure 4 inset. The anodic and cathodic peak currents were measured by one pair of redox peaks produced by the UTPtNWs, which have peak potentials of −0.18 and −0.16 V vs SCE, respectively. Both the anodic and cathodic peak currents were linearly proportional to $v^{1/2}$, suggesting a diffusion-limited redox process.

In conclusion, we have demonstrated a simple route for preparing high-quality Pt NWs with an ultrathin diameter of ∼1.8 nm and very high aspect ratios of >10^4. The key for the successful synthesis of these high-quality Pt NWs with very high aspect ratios is the use of INSAFs as sacrificial templates to control the morphology. The as-prepared UTPtNWs exhibited attractive electrocatalytic behavior, which is of special interest for a variety of applications. The use of UTPtNWs as catalysts should open new and exciting possibilities for enhancing the performance of electrochemical activity, and this nanostructure may also be useful in sensing, biomedical, and other electrochemical applications.

◼ ASSOCIATED CONTENT

Ⓢ Supporting Information

Experimental details, TEM image of INSAFs, XRD patterns of INSAFs and UTPtNWs, TEM images of UTPtNWs and a commercial Pt/C catalyst before and after 1000 CV scans, and a possible detailed mechanism of UTPtNWs growth. This material is available free of charge via the Internet at http://pubs.acs.org.

◼ AUTHOR INFORMATION

Corresponding Author
fmgao@ysu.edu.cn

Author Contributions
[†]L.Z. and N.L. contributed equally.

Notes
The authors declare no competing financial interest.

◼ ACKNOWLEDGMENTS

◼ REFERENCES

(1) (a) Davis, R. J.; Derouane, E. G. *Nature* **1991**, *349*, 313. (b) Bönnemann, H.; Brijoux, W.; Tilling, A. S.; Siepen, K. *Top. Catal.* **1997**, *4*, 217. (c) Shimada, T.; Nakamura, I.; Yamamoto, Y. *J. Am. Chem. Soc.* **2004**, *126*, 10546. (d) Diezi, S.; Ferri, D.; Vargas, A.; Mallat, T.; Baiker, A. *J. Am. Chem. Soc.* **2006**, *128*, 4048.

(2) Kolmakov, A.; Klenov, D. O.; Lilach, Y.; Stemmer, S.; Moskovits, M. *Nano Lett.* **2005**, *5*, 667.

(3) (a) Koenigsmann, C.; Santulli, A. C.; Gong, K.; Vukmirovic, M. B.; Zhou, W. P.; Sutter, E.; Wong, S. S.; Adzic, R. R. *J. Am. Chem. Soc.* **2011**, *133*, 9783. (b) Koenigsmann, C.; Zhou, W. P.; Adzic, R. R.; Sutter, E.; Wong, S. S. *Nano Lett.* **2010**, *10*, 2806. (c) Guo, S. J.; Wen, D.; Zhai, Y. M.; Dong, S. J.; Wang, E. K. *ACS Nano* **2010**, *4*, 3959.

(4) Williams, M. C. *Fuel Cells* **2001**, *1*, 87.

(5) (a) Subhramannia, M.; Pillai, V. K. *J. Mater. Chem.* **2008**, *18*, 5858. (b) Cademartiri, L.; Ozin, G. A. *Adv. Mater.* **2009**, *21*, 1013.

(c) Xia, Y. N.; Yang, P. D.; Sun, Y. G.; Wu, Y. Y.; Mayers, B.; Gates, B.; Yin, Y. D.; Kim, F.; Yan, H. Q. *Adv. Mater.* **2003**, *15*, 353.

(6) (a) Wang, C.; Waje, M.; Wang, X.; Tang, J. M.; Haddon, R. C.; Yan, Y. *Nano Lett.* **2004**, *4*, 345. (b) Chen, Z.; Waje, M.; Li, W.; Yan, Y. *Angew. Chem., Int. Ed.* **2007**, *46*, 4060.

(7) Sun, S.; Jaouen, F.; Dodelet, J. P. *Adv. Mater.* **2008**, *20*, 3900.

(8) Sun, S. H.; Zhang, G. X.; Zhong, Y.; Liu, H.; Li, R. Y.; Zhou, X. R.; Sun, X. L. *Chem. Commun.* **2009**, 7048.

(9) (a) Nielsen, L.; Khurana, R.; Coats, A.; Frokjaer, S.; Brange, J.; Vyas, S.; Uversky, V. N.; Fink, A. L. *Biochemistry* **2001**, *40*, 6036. (b) Jansen, R.; Dzwolak, W.; Winter, R. *Biophys. J.* **2005**, *88*, 1344. (c) Jiménez, J. L.; Nettleton, E. J.; Bouchard, M.; Robinson, C. V.; Dobson, C. M.; Saibil, H. R. *Proc. Natl. Acad. Sci. U.S.A.* **2002**, *99*, 9196. (d) Leroux, F.; Gysemans, M.; Bals, S.; Batenburg, K. J.; Snauwaert, J.; Verbiest, T.; Haesendonck, C. V.; Tendeloo, G. V. *Adv. Mater.* **2010**, *22*, 2193. (e) Hsieh, S. C.; Hsieh, C. W. *Chem. Commun.* **2010**, *46*, 7355. (f) Tang, Q.; Solin, N.; Lu, J.; Inganäs, O. *Chem. Commun.* **2010**, *46*, 4157. (g) Hsieh, C. W.; Hsieh, S. C. *J. Mater. Chem.* **2011**, *21*, 16900.

(10) (a) Serio, T. R.; Cashikar, A. G.; Kowal, A. S.; Sawicki, G. J.; Moslehi, J. J.; Serpell, L.; Arnsdorf, M. F.; Lindquist, S. L. *Science* **2000**, *289*, 1317. (b) Scheibel, T.; Lindquist, S. L. *Nat. Struct. Biol.* **2001**, *8*, 958. (c) DePace, A. H.; Weissman, J. S. *Nat. Struct. Biol.* **2002**, *9*, 389.

(11) Gómez, R.; Orts, J. M.; Álvarez-Ruiz, B.; Feliu, J. M. *J. Phys. Chem. B* **2004**, *108*, 228.

(12) (a) Kita, H.; Gao, Y.; Nakato, T.; Hattori, H. *J. Electroanal. Chem.* **1994**, *373*, 177. (b) Herrero, E.; Franaszczuk, K.; Wiechowski, A. *J. Phys. Chem.* **1994**, *98*, 5074. (c) Hamnett, A. *Catal. Today* **1997**, *38*, 445.